The Structure of Molten Rare-earth Iodide-Alkali Iodide Mixtures

Athanassios Chrissanthopoulos, Georgia D. Zissi, and George N. Papatheodorou

Foundation for Research and Technology Hellas - Institute of Chemical Engineering and High Temperature Chemical Processes (FORTH-ICE/HT), P. O. Box 1414, and Department of Chemical Engineering, University of Patras, GR-26504, Patras, Greece

Reprint requests to Prof. G. N. P.; E-mail: gpap@iceht.forth.gr

Z. Naturforsch. **60a,** 739 – 748 (2005); received August 2, 2005

The composition and temperature dependence of the Raman spectra of molten LnI_3-CsI (Ln = Ce, Dy, Ho) mixtures have been measured. Raman spectra of the polycrystalline compounds CeI_3, DyI_3, Cs_3CeI_6, Cs_3DyI_6 and $Cs_3Dy_2I_9$ have also been measured from room temperature up to ~ 750 °C, where melting occurs for most of these salts. The data are correlated to previous studies involving rare-earth chlorides and bromides and are discussed in terms of the melt structure and the structural systematics of the rare-earth iodide-alkali iodide molten mixtures.

Key words: Rare-earth Iodides; Molten Salts; Structure.

1. Introduction

The structural and thermodynamic properties of molten trivalent rare-earth halides and their binary compounds with alkali halides depend strongly on the physicochemical properties of the trivalent salt [1]. Detailed Raman spectroscopic measurements on a series of rare-earth-alkali halide mixtures LnX_3-AX (A= alkali metal; X = F, Cl, Br) [2, 3] indicate that the spectral behavior and structure of these melts are very similar, especially in the dilute rare-earth halide mixtures. In general two polarized bands P_1 and P_2 and two depolarized bands D_1 and D_2 appear in the spectra. The P_1 band does practically not change with composition, and its frequency is associated with the Ln-X vibration of the six-fold coordinated species. The P_2 band shifts continuously to higher frequencies with increasing LnX_3 content. This behavior is attributed to the formation of a weak network in the melt composed of distorted halide-sharing octahedra. Rather different is the behavior of the ScI_3-CsI [4] and $ScCl_3$-CsCl [5] systems, where multispecies equilibria involving ScX_6^{3-}, $Sc_2X_9^{3-}$, ScX_4^- appear to predominate the melt structure.

Studies of binaries containing high-melting lanthanide iodides are limited, mainly due to experimental difficulties. The practical interest for studying the iodide mixtures arises from their use as additives in high-intensity-discharge mercury lamps. In a metal halide lamp the dissociation of metal halides in the high temperature arcs and the recombination on the wall is a repeated procedure. Iodides are more suitable for this cycle as they have higher vapor pressures and lower decomposition temperatures than chlorides and bromides. It is very important to know the structure of the melt in order to fully understand and describe the vapor species and their chemistry inside the lamp [6].

In the present work the lanthanide iodide systems LnI_3-CsI (Ln = Ce, Dy and Ho) are investigated by Raman spectroscopy, and the results are discussed in terms of the melt structure and in correlation with the chloride and bromide systems studied so far. The structural trends of the rare-earth iodide systems are also discussed.

2. Experimental

Caesium iodide (Fluka, 99.99%) was dehydrated by heating gradually up to 300 °C under vacuum for several hours. Cerium(III), dysprosium(III) and holmium(III) iodides (APL Engineered Materials Inc., 99.99%) were first heated gradually up to 500 °C under vacuum for several hours and then sealed in long quartz tubes and heated up to 950 °C. All anhydrous materials were handled in the inert atmosphere of a glove box having a water content of less than 1 ppm. The experimental setup for Raman measurements at elevated temperatures has been described in [4, 5]. The 514.5 and 647.1 nm lines of Ar and Kr ion Spectra Physics lasers

were used. The spectral resolution was $1-2$ cm^{-1} for solid and 4 cm^{-1} for liquid samples.

Fused silica cylindrical cells ($\sim$ 4 mm O. D., $\sim$ 3 mm I. D., $\sim$ 2 cm length) were used for recording the Raman spectra. Two polarization configurations, VV and HV, were measured in a 90° scattering geometry. The digitally stored data were used for the calculation of the isotropic, anisotropic and reduced representations of the spectra [1, 2]. Cells having different compositions were prepared and the spectra were measured at different temperatures above the binary liquidus and up to $\sim$ 750 °C. Two problems were encountered: The extended contact of the LnI_3-rich mixtures with the silica cell caused corrosion at high temperatures and the melts were colored (from f←f and charge transfer, CT, electronic transitions) and this led to partial absorption of the laser excitation lines. The best line to use was the 647.1 nm Kr line, which was less absorbed by the sample. With increasing temperature the tail of the CT band covered lower energies, the absorption increased and the scattering intensity diminished. Furthermore, above 750 °C the furnace's black body radiation in the 647.1 nm region increased, and this in combination with the low intensities due to the laser absorption gave very low S/N ratio spectra and no measurements were possible.

It was possible, however, to measure the CeI_3-CsI spectra in the complete composition range, while for the higher melting and higher laser absorbing system DyI_3-CsI spectra were only measured up to 55 mol% DyI_3. The 50/50 HoI_3-CsI melt mixture was also measured. The solid compounds Cs_3CeI_6, Cs_3DyI_6 and $Cs_3Dy_2I_9$ were prepared by mixing in the Raman cells the appropriate amounts of the iodides according to the phase diagrams [7].

The melts were then cooled to room temperature, and the spectra were measured directly from the bulk polycrystalline solids in the cells.

3. Results and Discussion

3.1. General

Spectra from more than 15 different cells containing different melt compositions were measured from room temperature up to the melting points or above the corresponding liquidus temperatures. The solids placed in the cell were first melted and then cooled to room temperature. The spectra of the solid mixtures obtained this way were found to be a superposition of Raman bands of the component solids found in the phase diagrams [7] and are not worth reporting. On the other hand the spectra of the well defined compounds in the phase diagrams have been studied including the pure lanthanide iodide solids. In the following results from the molten mixtures and solid compounds are presented and discussed. Two types of spectra representations are used; the raw Raman spectra and the calculated reduced Raman spectra. Details for calculating the reduced representations and the advantages of using them can be found in [1].

3.2. The Melting of the Binary Compounds

A large number of phase diagrams of the type LnI_3-AI (Ln = lanthanide, A = alkali metal) have been measured over the years [7]. The systematics of binary compound formation in these systems have also been studied [8–10]. All the systems LnI_3-CsI (Ln = Nd to Lu, Y and Sc) show the presence of two compounds with well defined melting points: Cs_3LnI_6 and $Cs_3Ln_2I_9$. The CeI_3-CsI phase diagram has to our knowledge not been measured yet, but phase diagrams of the neighboring systems LaI_3-CsI and PrI_3-CsI are known, and both show the formation of only the Cs_3LnI_6 compound, while the $Cs_3Pr_2I_9$ compound is formed at a peritectic melting point. This indicates that for the CeI_3-CsI binary system the only compound formed should be Cs_3CeI_6. The phase diagram of the DyI_3-CsI system, however, shows the compounds Cs_3DyI_6 (m. p. $\sim$ 715 °C) and $Cs_3Dy_2I_9$ (m. p. $\sim$ 643 °C).

The crystal structures of Cs_3CeI_6 and Cs_3DyI_6 are not known, but from the systematics of the binary compounds "one can be quite certain that both exhibit octahedral surroundings of the Ln cation" [10]. A phase transition at $\sim$ 484 °C occurs for the Cs_3DyI_6, and a similar transition is expected for the corresponding Ce compound. The Raman spectra of these two polycrystalline solids are shown in Figs. 1a and 1b. They are very similar, indicating that these compounds are isomorphous. At elevated temperatures the two well defined bands are assigned as before [1–3] to the $\nu_1(A_{1g})$ and $\nu_5(T_{2g})$ modes of the LnI_6^{3-} octahedra existing as "isolated" ionic species within the solid. Upon melting the vibrational modes of LnI_6^{3-} are transferred into the liquid. The changes seen for both compounds follow the systematics observed for a large number of A_3LnX_6 solids [1–3] and support the view that the predominant species formed in the melt are the LnI_6^{3-} octahedra. The ν_1 mode in the melt is marked as P_1,

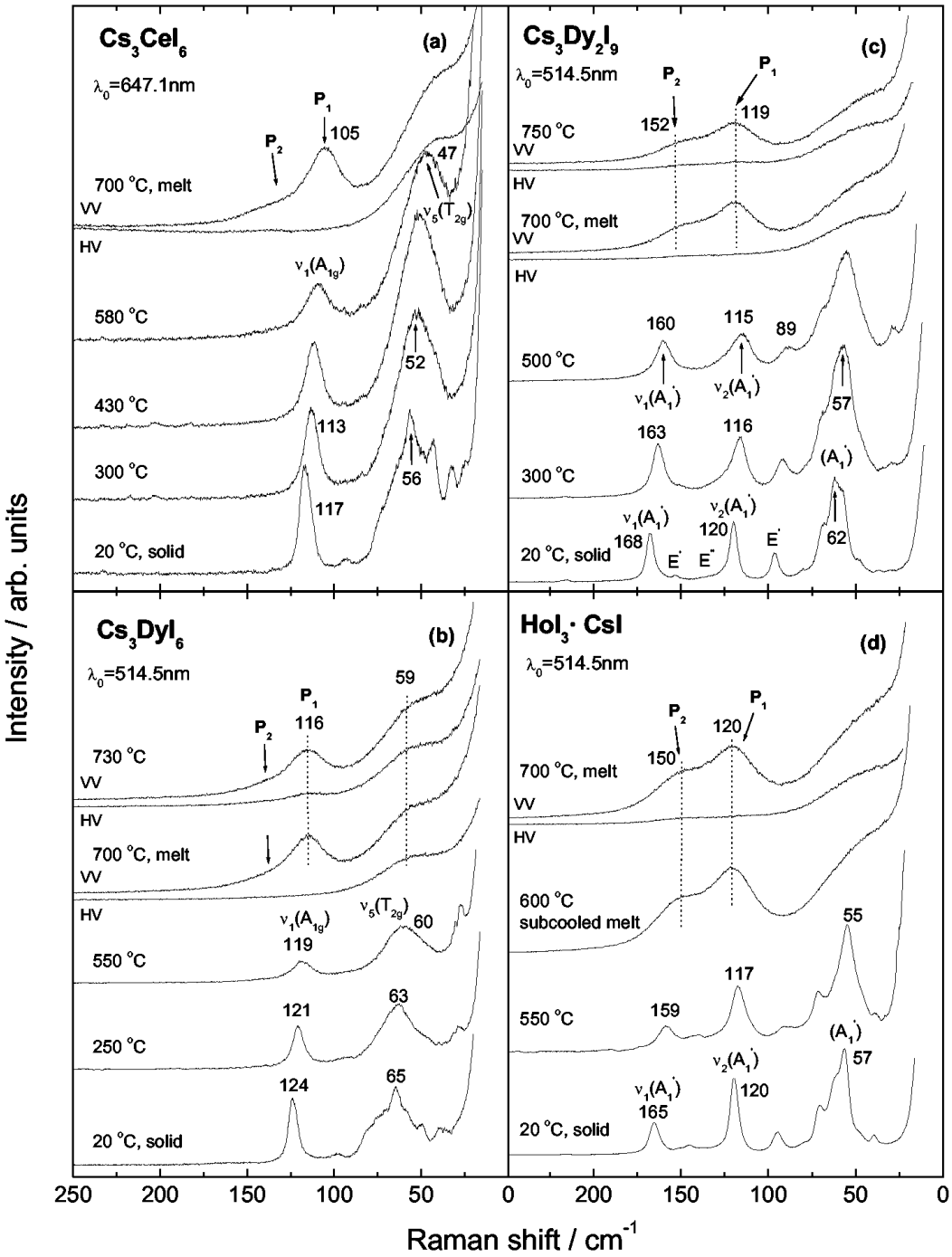

Fig. 1. Temperature dependence of solids and melts. (a), (b) The Cs_3LnI_6 compounds: $\nu_1(A_{1g})$ and $\nu_5(T_{2g})$ are the two more intense Raman active modes of the LnI_6^{3-} octahedra; (c) the $Cs_3Dy_2I_9$ compound: assignments based on the $Dy_2I_9^{3-}$ "molecular" ion; (d) the $HoI_3 - CsI$ (1:1) mixture: the solid consists of a mixture of $Cs_3Ho_2I_9$ ($\sim$ 80 mol%) and HoI_3 ($\sim$ 20 mol%), and the main bands seen are those of the $Ho_2I_9^{3-}$ "molecular" ion as in Fig. 1c. Spectral conditions: for (a) $\lambda_0 = 647.1$ nm, power = 180 mW; for (b), (c) and (d) $\lambda_0 = 514.5$ nm, power = 1 W. The resolution is $1-2$ cm^{-1} for solids and 4 cm^{-1} for liquids, scan rate = 0.8 cm^{-1} s^{-1}.

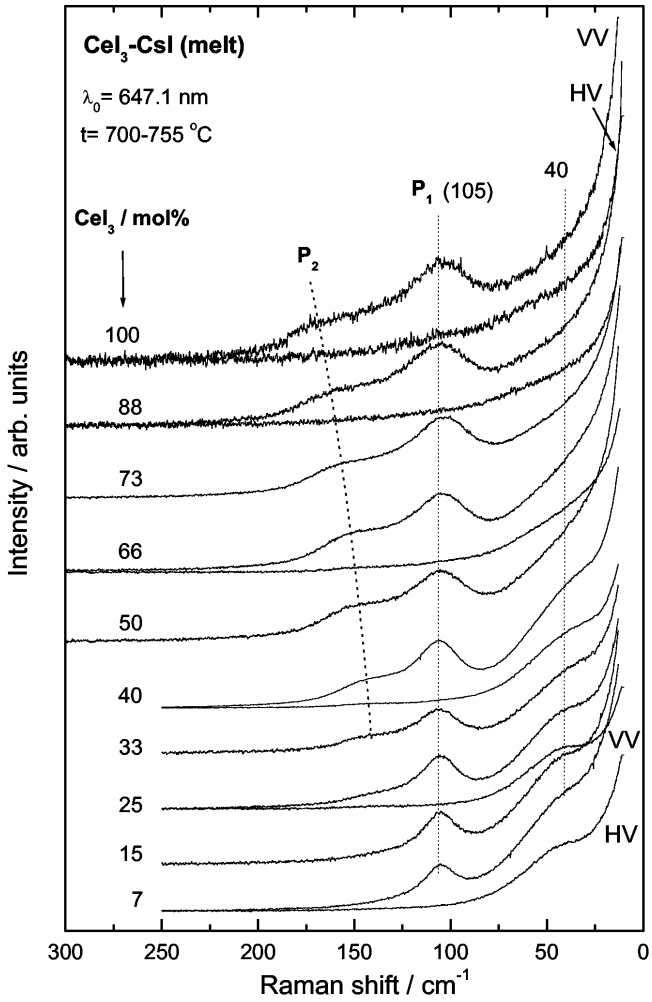

Fig. 2. Composition dependence of the raw Raman spectra of CeI_3-CsI molten mixtures. Up to 73 mol% CeI_3 the spectra were measured at 700 °C. For 88 and 100 mol% CeI_3 the temperatures were above the liquidus 720 and 755 °C, respectively. Spectra conditions: $\lambda_0 = 647.1$ nm, power = 180 mW; resolution is 4 cm^{-1}, scan rate = 0.8 cm^{-1} s^{-1}. For each composition the upper spectrum is VV and the lower HV. For clarity certain HV spectra are omitted.

while a second rather weak band P_2 is also present. Variation of temperature does not change the relative intensities (Fig. 1b) which indicates a rather stable predominant melt structure. The independence of the spectra on the temperature is discussed in more detail in the following subsection.

Crystalline $Cs_3Dy_2I_9$ is known [11] to be isomorphous to $Cs_3Y_2I_9$ which has $P6_3/mmc\,(D^4_{6h})$ space group symmetry [4]. In these compounds $Ln_2X_9^{3-}$ "molecular" ions are formed, having two octahedra bound by a face. Their Raman spectra are dominated by the vibrational modes of $Ln_2X_9^{3-}$ which span the representation: $\Gamma(D_{3h}) = 4A'_1 + 5E' + 4E''$. Figure 1c shows the temperature dependence of the $Cs_3Dy_2I_9$ solid spectra and the assignments of the main bands based on the previous Raman study of the isomorphous $Sc_2Cl_9^{3-}$ ion [12]. Upon melting the spectra of $Cs_3Dy_2I_9$ change, showing the polarized bands P_1 and P_2 and a broad depolarized band. Increasing temperature does not affect the relative intensities of the P_1 and P_2 bands. The situation differs from that found for the $Cs_3Sc_2Cl_9$ melts [5, 12], where drastic intensity changes occur with the temperature, indicating the presence of multispecies equilibria (see also the following subsection). Thus, the polarized melt spectra of $Cs_3Dy_2I_9$ are dominated by the P_1 band which, as in the case of Cs_3LnI_6 melts, is assigned to the DyI_6^{3-}, ν_1, octahedral mode, and by the P_2 band whose origin is further discussed below.

3.3. Composition and Temperature Effects

The raw Raman spectra of the CeI_3-CsI and DyI_3-CsI melt mixtures measured at different compositions are shown in Figs. 2 and 3, respectively. The spectra

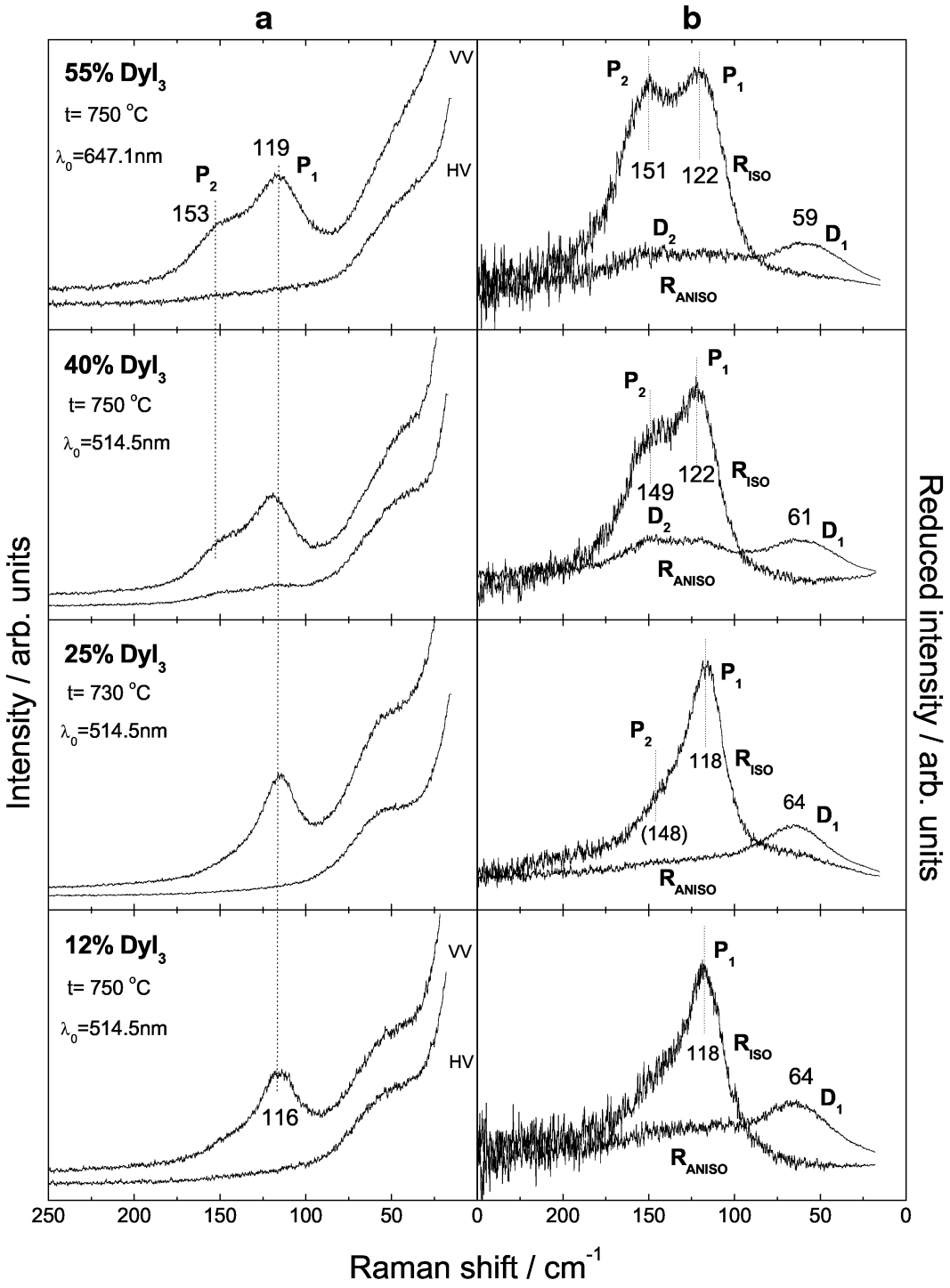

Fig. 3. Composition dependence of the Raman spectra of DyI_3-CsI molten mixtures. Left column: VV and HV data; right column: reduced isotropic (R_{ISO}) and anisotropic (R_{ANISO}) spectra. Spectra conditions: $\lambda_0 = 514.5$ nm, power = 0.5 – 1 W, resolution = 4 cm^{-1}, scan rate = 0.8 cm^{-1} s^{-1}.

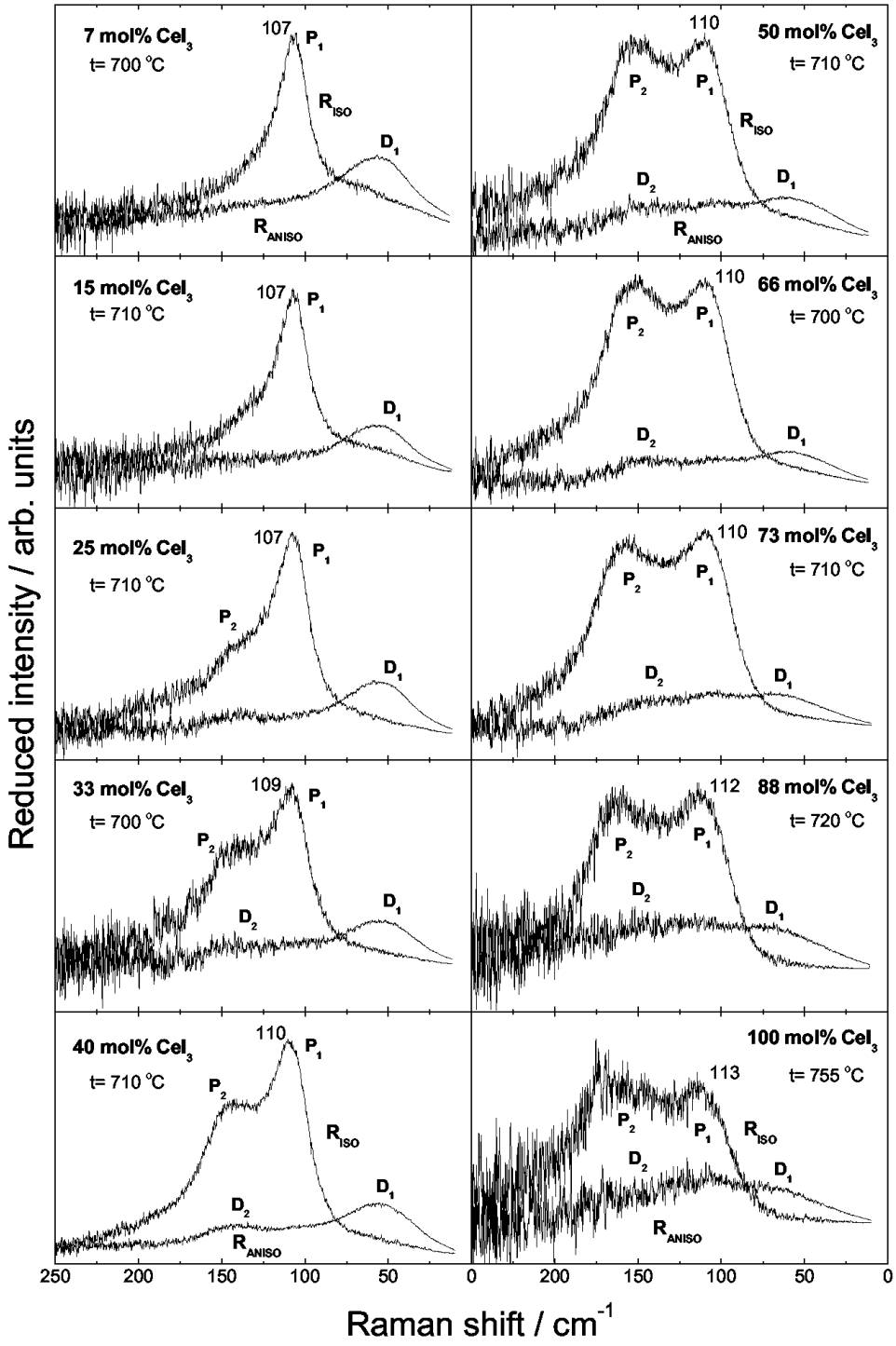

Fig. 4. Composition dependence of the reduced isotropic (R_{ISO}) and anisotropic (R_{ANISO}) Raman spectra of CeI_3-CsI molten mixtures. Spectral conditions are as in Figure 2. The low S/N ratio at high frequencies is due to the amplification of the base line noise by the calculation of the reduced representation (details of calculation in [1]).

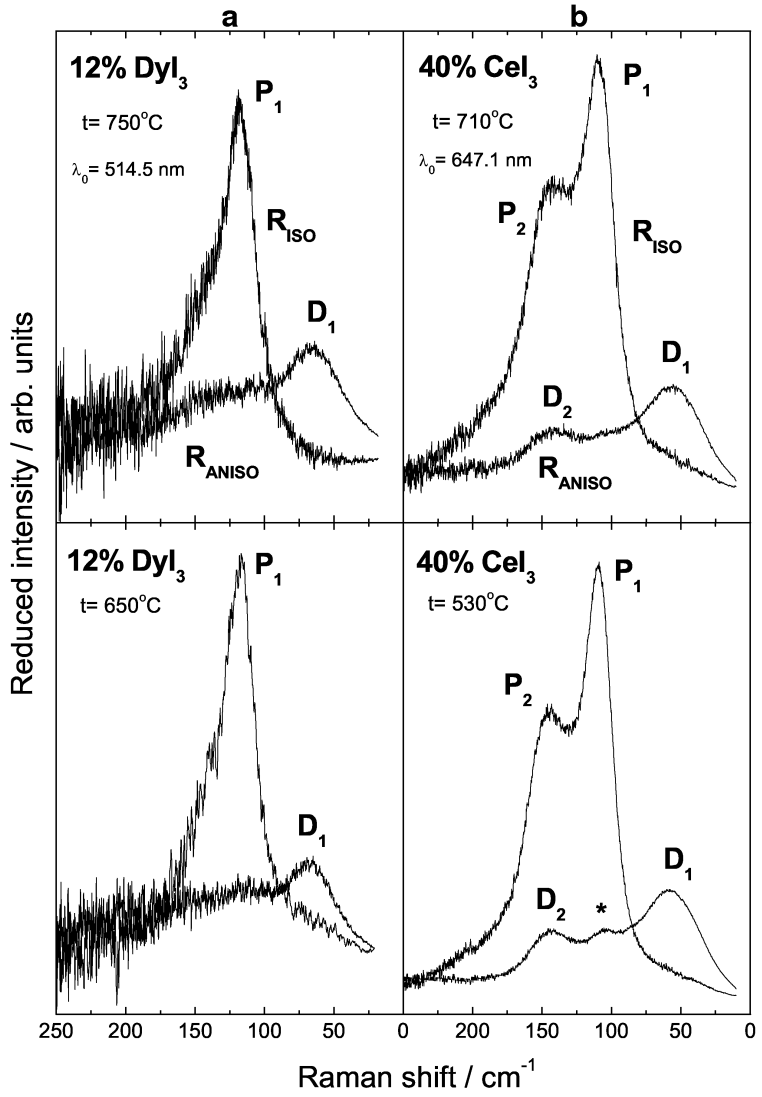

Fig. 5. Temperature dependence of the reduced isotropic (R_{ISO}) and anisotropic (R_{ANISO}) Raman spectra of "low" melting LnI_3-CsI mixtures: (a) 12 mol% DyI_3, spectral conditions as in Fig. 3; (b) 40 mol% CeI_3, spectral conditions as in Figure 2. Spectra at intermediate temperatures have been also measured but showed no temperature effect. The * denotes linkage of polarized light due to partial misalignment of the cell.

of corresponding compositions in the two figures are "isomorphous", indicating that similar structures exist in both molten mixtures. The P_1 band is present at all compositions, while the P_2 band becomes distinct at $x_{LnI_3} > 0.25$ and shifts gradually to higher frequencies with increasing LnX_3 mole fraction. The depolarized bands are best seen in the reduced representation [1] of the spectra, which are shown for the CeI_3-CsI system in Fig. 4 and for the DyI_3-CsI system in Figure 3b. Thus, the overall spectra are characterized by the two polarized bands P_1 and P_2 plus the depolarized bands D_1 and D_2. The systematic changes occurring with mole fraction variation are the same to those observed in a series of rare-earth chlorides [1, 2] and bromides [3], and the band assignments and melt structure for all these systems should be similar. The P_1 band corresponds to the LnI_6^{3-} octahedral stretching frequency, which does practically not change as we go from the CsI-rich to the LnI_3-rich melt. Increasing the LnI_3 mole fraction above 0.25 imposes sharing of common iodides between the lanthanide cations, thus forming distorted octahedral structures bridged to each other in a loose network-like structure [1 – 5]. The origin of the P_2 band is as before attributed to: (i) either splitting of the octahedral vibrational states due to the gradual distortions towards lower symmetries (i. e. C_{3v}, D_3) [1 – 3] or (ii) an induced hyperpolarizability mechanism that activates (the otherwise Raman inactive)

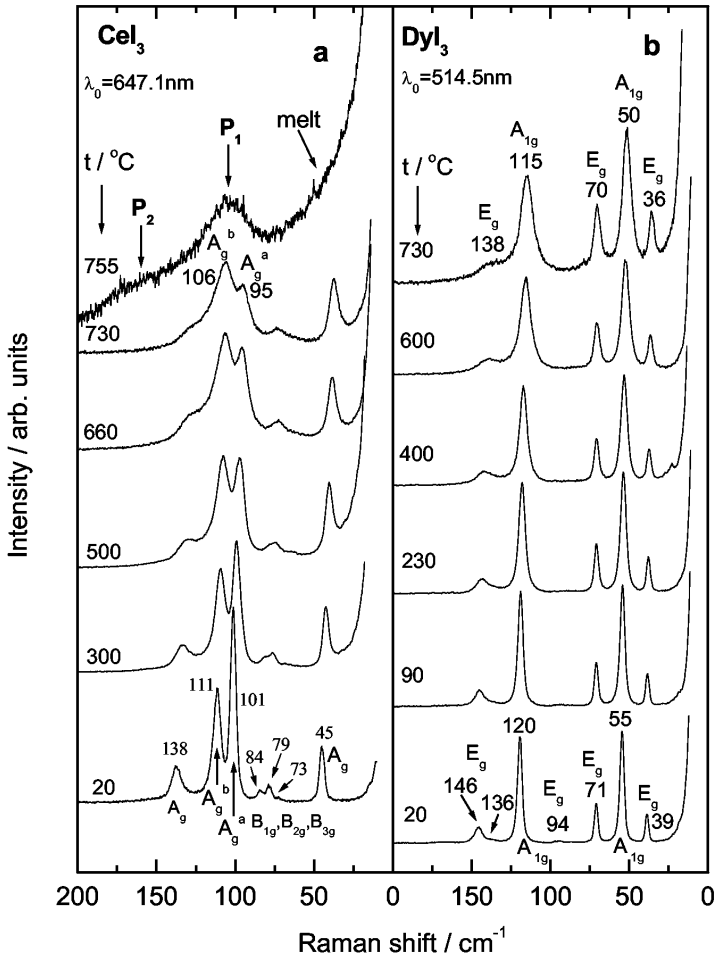

Fig. 6. Temperature dependence of the raw Raman spectra of solid: (a) CeI_3 and (b) DyI_3. Spectral conditions as in Fig. 1a and 1b, respectively. The CeI_3 melt spectra are the same as in Figs. 2 and 4.

asymmetric stretching modes of the distorted octahedra [13]. As pointed out in [5], both interpretations for the P_2 band are rather equivalent. An account of the D_1 and D_2 bands is also given by the gradual distortion/splitting mechanism [1–3].

The Raman spectra of the HoI_3-CsI (50/50) mixture were also measured (Fig. 1d). The phase diagram of the system shows that at this composition the solidified melt gives a solid, predominated by the $Cs_3Ho_2I_9$ compound. Thus, as seen in Fig. 1d, the solid spectra are "isomorphous" to those of $Cs_3Dy_2I_9$ (Fig. 1c), and upon melting the P_1, P_2 set of bands appears for both systems. In other words, the spectra of all three binary melts LnI_3-CsI (Ln = Ce, Dy, Ho) have common characteristics, leading to the conclusion that the melt structures are similar and can be described with the octahedral distortion scheme and the loose network-like structure of bridged octahedra [1–3].

Supporting this scheme are the temperature dependence measurements of the Raman spectra shown in Fig. 5 and on the top of Figs. 1b, 1c and 1d. For all compositions studied there exist practically no spectral changes with temperature. The importance of this observation can be better understood and appreciated by comparing the present spectra with those of the $ScCl_3$-CsCl [5] and the ScI_3-CsI [4] systems, where vast changes occur with temperature, revealing the presence of equilibria involving different anionic species. Thus, for the 12 mol% $ScCl_3$ molten binary two species $ScCl_6^{3-}$ and $ScCl_7^{-4}$ have been detected [5, 14] from two Raman bands, whose intensities are affected by temperature. Clearly such changes are not seen in the 12 mol% DyI_3 system (Fig. 6). Furthermore, the 40 and 50 mol% $ScCl_3$ (or ScI_3) spectra show drastic variation of the relative Raman intensities with temperature which presumably is due to an equilibrium involv-

ing the $ScCl_6^{3-}$, $Sc_2Cl_9^{3-}$ and $ScCl_4^-$ species [4, 5, 12]; no such changes are seen in the spectra of the systems studied here at the corresponding compositions shown in Figs. 1c, 1d and 5. These observations indicate that for all three systems LnI_3-CsI (Ln = Ce, Dy, Ho) the predominant vibrational modes are not affected by temperature variation. This implies that the octahedral network-like structure remains stable at all temperatures.

3.4. Temperature Dependence of Raman Spectra of Solid CeI$_3$ and DyI$_3$

The crystal structures of the lanthanide iodides are dominated by two space groups. The lighter (La - Nd) lanthanide iodides are orthorhombic, and are isostructural to $PuBr_3$ [$Cmcm\,(D_{2h}^7)$] [15] having the Ln^{3+} cation in an eight-fold coordination [$LnI_{6/3}I_{2/2}$] with six iodides shared by three cations and two iodides shared by two cations. The predicted Raman active bands are $\Gamma(D_{2h}^{17}) = 4A_g + 3B_{1g} + B_{2g} + 4B_{3g}$. The heavier (Sm - Lu) lanthanide iodides are rhombohedral and are isostructural to BiI_3 ($C_{3i}^2 - R\bar{3}$) [16] having the Ln^{3+} cation in distorted octahedral coordination [$LnI_{6/3}$] involving octahedral edge bridging. The predicted Raman active modes are $\Gamma(C_{3i}^2) = 4A_g + 4E_g$, but it has been shown that the spectra are dominated by the modes of edge bridged octahedra forming layers (D_{3d}^1 symmetry) within the crystal [17]: $\Gamma(D_{3d}^1) = 2A_{1g} + 4E_g$.

Figure 6 shows the Raman spectra of CeI_3 and DyI_3, each representing the light and the heavy lanthanide iodide group, respectively. The assignments given in the figure correspond to the above representations and the Raman work on the isostructural PmX_3 (X = F, Cl, Br, I) compounds [18]. The effect of temperature on the vibrational modes of solid DyI_3 shows the expected band broadening, and the frequency shifts to lower energies. At high temperatures the dominant vibrational modes are those due to the above mentioned substructures of the bridged octahedral layers. Over the temperature range studied no changes of the relative band intensities occurred.

The room temperature spectrum of CeI_3 is dominated by the four A_g modes, as it has been previously seen in the spectra of $NdBr_3$ [3], o-PmI_3 and $PmBr_3$ [18]. Increasing temperature broadens the bands and shifts them to lower energies. At the same time the intensities of the ~ 100 cm^{-1} ($A_g{}^a$) and 110 cm^{-1} ($A_g{}^b$) bands change relative to each other and to the other two A_g bands, which appear to have a constant intensity ratio. At 500 °C the $A_g{}^a$ and $A_g{}^b$ intensities are about equal as in the spectra of o-PmI_3, while at ~ 730 °C the intensity ratio is similar to that of the $PmBr_3$ spectra. There is no obvious explanation of the intensity changes seen. The effect is continuous with temperature and reversible, which indicates that this might be the beginning of a second order phase transition. In the eight-fold local coordination $CeI_{6/3}I_{2/2}$ the six iodides form octahedra, and each iodide is three-fold coordinated with Ce^{3+} (i. e. triple-bridged), while the remaining two iodides are two-fold coordinated with Ce^{3+} (i. e. double-bridged). The Ce-I distances of the triple-bridged iodides are slightly longer (3.08 Å) than that of the double-bridged (3.06 Å). With increasing temperature the amplitudes of vibration increase and should have a tendency to equalize the Ce-I distances, creating a more uniform eight-fold coordination for the Ce^{3+}. Thus a gradual structural change may occur which could be interpreted as a predisposition towards a second order phase transition.

Upon melting CeI_3, the polarized P_1, P_2 and the depolarized D_1, D_2 (Figs. 4 and 6) bands are formed. The three high frequency A_g bands of the solid are covered by the P_1 band with a maximum centered between the $A_g{}^a$ and $A_g{}^b$ bands. On the other hand the frequency of the P_2 band is by about 30% higher than that of the A_g band at ~ 130 cm^{-1} which is the highest frequency band of the solid. In this respect it seems that there is no correspondence between the high temperature solid and the melt spectra.

4. Conclusion

In the present work Raman spectroscopy has been used to study different compositions of molten LnI_3-CsI (Ln = Ce, Dy, Ho) mixtures. The spectral behavior for all three systems follows a pattern similar to that observed previously for other LnX_3-AX (A = alkali metal, X = Cl, Br) systems [1 – 3]. A predominant polarized band P_1 is present at all compositions and is assigned to the LnI_6^{3-} "octahedral" stretching mode. A second polarized band P_2 is also present, whose position shifts continuously to higher frequencies with increasing LnI_3 mole fraction. This overall behavior in conjunction with the spectra invariability with temperature suggests that the "octahedral" network-like structural model suggested for the chlorides and bromides [1] is also applicable for the studied iodide sys-

tems. Furthermore, since the lanthanide iodides examined here are either in the beginning (CeI_3) or towards the end (DyI_3, HoI_3) of the lanthanide series, it is more likely that all the lanthanide iodide-alkali iodide melts possess a common structural behavior. Due to the almost identical ionic size of Ho^{3+} and Y^{3+}, the YI_3-AI systems should also behave similarly. On the other hand, as it has been shown before [4], the structure of the ScI_3-CsI melt mixtures follow a different behavior, which is similar to that of the $ScCl_3$-CsCl system [5]. By changing CsI with the lighter alkali metal iodides (e.g. LiI) the overall structural behavior would be analogous to that found for example for the $NdBr_3$-LiBr [3] or YCl_3-LiCl [2] systems. Thus the predominant species in Li-rich melts would be LnI_6^{3-} having a highly distorted octahedral geometry and shorter life times due to the high polarizing power of its neighboring Li^+ cations. On the other hand, in LnI_3-rich melts the structure would not be much influenced by the size of the counter alkali metal cation. Finally it should be emphasized that in support of the above systematics derived from the spectroscopic measurements, are the enthalpy of mixing data on a series of lanthanide halides–alkali halides melt mixtures [19].

[1] G. N. Papatheodorou and S. N. Yannopoulos, Light Scattering from Molten Salts: Structure and Dynamics, NATO Science Series II, Molten Salts: From Fundamental to Applications (Ed. M. Gaune-Escard), Kluwer Academic Publishers, Dordrecht 2002, Vol. 52, p. 47.
[2] G. N. Papatheodorou, J. Chem. Phys. **66**, 2893 (1977).
[3] G. M. Photiadis, B. Børresen, and G. N. Papatheodorou, J. Chem. Soc., Faraday Trans. **94**, 2605 (1998) and references therein.
[4] M. M. Metallinou, L. Nalbandian, G. N. Papatheodorou, W. Voigt, and H. H. Emons, Inorg. Chem. **30**, 4260 (1991).
[5] G. D. Zissi and G. N. Papatheodorou, Phys. Chem. Chem. Phys. **6**, 4480 (2004).
[6] A. Chrissanthopoulos, G. D. Zissi, and G. N. Papatheodorou, Inst. Phys. Conf. Ser. **182**, 267 (2004).
[7] Phase Diagrams for Ceramists, American Ceramic Society, Westerville, OH, Vols. V (1983) and VII (1989).
[8] (a) J. Kutscher and A. Schneider, Z. anorg. allg. Chem. **386**, 38 (1971); (b) J. Kutscher, Ph. D. Thesis, Technical University of Clausthal 1972.
[9] H. J. Seifert, J. Therm. Anal. Calor. **67**, 789 (2002).
[10] G. Meyer, Prog. Solid State Chem. **14**, 141 (1982).
[11] M. Lenck and A. Weiss, Z. Naturforsch. **47a**, 54 (1992).
[12] G. D. Zissi and G. N. Papatheodorou, Chem. Phys. Lett. **308**, 51 (1999).
[13] P. A. Madden, M. Wilson, and F. Hutchinson, J. Chem. Phys. **120**, 6609 (2004).
[14] G. D. Zissi and G. N. Papatheodorou, J. Chem. Soc. Dalton Trans., 2599 (2002).
[15] (a) F. Weigel and V. Sherer, Radiochim. Acta **7**, 40 (1967); (b) J. R. Peterson, J. Alloys Comp. **223**, 180 (1995).
[16] D. Brown, Halides of the Lanthanides and Actinides, Wiley-Interscience, New York 1968.
[17] V. M. Bermudez, Solid State Commun. **19**, 693 (1976).
[18] W. R. Wilmarth, G. N. Begun, R. G. Haire, and J. R. Peterson, J. Raman Spectrosc. **19**, 271 (1988).
[19] (a) L. Rycerz and M. Gaune-Escard, Z. Naturforsch. **57a**, 136 (2002); (b) M. Gaune-Escard, A. Bogacz, L. Rycerz, and W. Szczepaniak, Thermochim. Acta. **279**, 51 (1996); (c) M. Gaune-Escard, A. Bogacz, L. Rycerz, and W. Szczepaniak, Thermochim. Acta. **236**, 67 (1994).